

Validity of rate equation results for reaction rates in reaction networks with fluctuations

Adina Lederhendler and Ofer Biham

Racah Institute of Physics, The Hebrew University, Jerusalem 91904, Israel

(Received 25 May 2008; revised manuscript received 8 September 2008; published 2 October 2008)

Systems of reacting particles, which are well mixed or distributed homogeneously in space, are commonly modeled by deterministic rate equations. These equations, which are based on the mean-field approximation, are valid for macroscopic systems. However, they neglect fluctuations in the particle populations. As a result, under conditions of strong fluctuations, the reaction rates obtained from the rate equations are highly inaccurate. To account for the fluctuations, stochastic methods are required. However, these methods are computationally intensive and may become infeasible for complex reaction networks. Therefore, it is useful to identify the conditions under which the rate equations provide accurate results. Naively, one expects strong fluctuations when the average population sizes of some of the reactants are of order one or lower. Here we present a systematic approach, for testing the validity of the rate equations, in which we define characteristic scales in terms of the rate constants of the network. We show that the rate equations fail to accurately reproduce the reaction rates when the system size is reduced below these scales. Surprisingly, the rate equations are found to be applicable in a wider range than expected. Their validity depends not only on the population sizes of the reactive species but also on the kinetic properties of the reaction network.

DOI: [10.1103/PhysRevE.78.041105](https://doi.org/10.1103/PhysRevE.78.041105)

PACS number(s): 02.50.Fz, 02.50.Ey, 02.70.Uu

I. INTRODUCTION

Systems of interacting species are prevalent in many fields of science, including chemistry, biology, and ecology. Such systems can be described by networks or graphs, in which each node represents a species and each edge represents an interaction. The interactions affect the population sizes of the different species, which may vary as a function of time. A common approach for the quantitative analysis of such systems is based on rate equations, which describe the temporal evolution of the population size of each species [1,2]. The rate equations are deterministic in the sense that they are based on a mean-field approach, which ignores stochastic effects. Thus, they are easy to construct and highly efficient in terms of computational resources. They provide accurate results when the populations are large and well mixed such that spatial inhomogeneities can be ignored. However, the rate equation method fails when features such as the discrete nature of the interacting species and fluctuations in their populations become important. Such situations are common in chemical and biological processes. For example, in surface catalysis systems, the surface is often partitioned into facets on nanometric dimensions, with little diffusion between the facets. Under these conditions the number of reactive atoms and molecules residing on a facet is small and fluctuations are strong [3–8]. Another important example of chemical reaction networks that require stochastic analysis appears in the field of interstellar chemistry [9–11]. Some of the chemical reactions in interstellar clouds take place on the surfaces of dust grains [12,13]. These include molecular hydrogen formation [14–17] as well as reaction networks that form ice mantles and certain organic molecules. Due to the submicron size of the grains and the low gas density, the populations of reactive species per grain are small and strongly fluctuate. Therefore, rate equations are not suitable for the evaluation of reaction rates in these systems [18–21]. Stochastic fluctuations also turn out to play an

important role in biochemical networks in living cells [22–24]. Recent advances in quantitative measurements of gene expression at the single-cell level enable to analyze these fluctuations and to examine their effect on cell function [25,26].

To obtain accurate results in simulations of strongly fluctuating networks of interacting species, one needs to use stochastic methods. Such methods can be implemented either by the direct integration of the master equation [27–31] or by Monte Carlo simulations [32–35]. However, these methods are computationally expensive. For example, the master equation is useful for the simulation of simple chemical reaction networks, which involve a small number of reactive species. However, as the number of chemical species increases, the number of coupled equations quickly proliferates. This makes the master equation infeasible for complex reaction networks [36,37]. Monte Carlo methods are also limited by the need to accumulate large amounts of statistical data in order to obtain accurate values for the average population sizes and reaction rates. Therefore, efforts have been made to develop efficient approximations of the master equation [38–47]. For example, the method presented in Refs. [41–43] is based on dimensional reduction of the master equation. The method of Refs. [44–46] is based on moment equations derived from the master equation, using a suitable truncation. Recently, hybrid methods [48–50] which dynamically apply either stochastic or deterministic methods, have been introduced.

The question of identifying the crossover of a system from deterministic to stochastic behavior is of general importance. Both the accuracy and efficiency of the simulation of a particular system may be considerably improved by using the most appropriate simulation method for given conditions. The rate equation method is advantageous in the deterministic case, while the stochastic methods are required when the system exhibits large fluctuations. In practice, the simulation method is often chosen according to insight obtained through trial and error. However, recent efforts have been made in

order to formulate more rigorous rules for the selection of the most appropriate simulation method [51]. In many cases one is primarily interested in the average population sizes of the interacting species and the reaction rates. It would thus be beneficial to formulate guidelines for the conditions under which the rate equations can be used to accurately calculate these quantities.

In this paper we formulate criteria for the validity of the rate equations for the calculation of reaction rates in reaction networks under steady-state conditions. To this end, we consider a class of spatially homogenous (well-mixed) systems involving n distinct species, labeled X_i , $i=1, \dots, n$. Particles of each species are introduced into the system at a rate G_i (s^{-1}), referred to as the generation rate. Each particle spontaneously degrades or leaves the system after an average lifetime of $t_i=1/D_i$, where D_i (s^{-1}) represents the degradation rate of an X_i particle. In addition, pairs of particles may encounter each other and react. The reaction rate between a pair of particles of species X_i and X_j is denoted by K_{ij} (s^{-1}).

The expressions used in order to calculate the average reaction rates highlight the fundamental differences between the rate equation approach and the stochastic approach. The rate equation method is based on the mean-field approximation, which identifies the instantaneous population size, N_i , of species X_i , with the ensemble average $\langle N_i \rangle$. According to this assumption, the average number of distinct pairs of X_i and X_j particles in the system is $\langle N_i \rangle \langle N_j \rangle$. Therefore, the reaction rate between particles of these two species is given by

$$R_{ij} = \begin{cases} K_{ii} \langle N_i \rangle^2 & \text{for } i=j, \\ K_{ij} \langle N_i \rangle \langle N_j \rangle & \text{for } i \neq j. \end{cases} \quad (1)$$

In the stochastic approach, the actual number of particles of each species which are simultaneously present in the system is taken into account. Consequently, the reaction rates in the stochastic approach are

$$R_{ij} = \begin{cases} K_{ii} \langle N_i(N_i-1) \rangle & \text{for } i=j, \\ K_{ij} \langle N_i N_j \rangle & \text{for } i \neq j. \end{cases} \quad (2)$$

Note that in the expressions for R_{ii} , a factor of 1/2 was integrated into the rate constant K_{ii} . The temporal evolution of the average particle populations can be described by the general equation

$$\langle \dot{N}_i(t) \rangle = G_i - D_i \langle N_i(t) \rangle - 2R_{ii}(t) - \sum_{j \neq i} R_{ij}(t) + \sum_{i+} R_{i+}(t), \quad (3)$$

where $i=1, \dots, n$. The first and second terms in Eq. (3) describe the addition and degradation of X_i particles, respectively. The third and fourth terms represent the removal of X_i particles by reactions. The last term accounts for all the processes in which X_i particles are formed. Equation (3) is applicable to both deterministic and stochastic calculations, depending on the form of the reaction terms R , as described above.

The paper is organized as follows. In Sec. II we consider a simple dimerization reaction and identify the range of parameters in which strong fluctuations render the rate equations invalid. In Sec. III we introduce the system-size ap-

proach, in which the boundary between the deterministic and stochastic regimes in the parameter space is derived in a more systematic fashion. This approach enables us to broaden the analysis to more complex reaction systems, as shown in Sec. IV. The results are discussed and summarized in Sec. V.

II. SINGLE SPECIES NETWORK

The simplest reaction network consists of a single reactive species X_1 , which undergoes dimerization $X_1 + X_1 \rightarrow X_2$. For simplicity we assume that the X_2 molecules do not take part in further reactions. In this case the network can be described by a single rate equation [52]

$$\langle \dot{N}_1 \rangle = G_1 - D_1 \langle N_1 \rangle - 2K_{11} \langle N_1 \rangle^2. \quad (4)$$

A more complete description of the system is given by the master equation, which expresses the temporal evolution of the probability $P_t(N_1)$ of finding exactly N_1 particles in the system at time t . For the single-species system, the master equation takes the form [27,28,53]

$$\begin{aligned} \dot{P}(N_1) = & G_1 [P(N_1-1) - P(N_1)] + D_1 [(\dot{N}_1+1)P(N_1+1) \\ & - N_1 P(N_1)] + K_{11} [(N_1+2)(N_1+1)P(N_1+2) \\ & - N_1(N_1-1)P(N_1)], \end{aligned} \quad (5)$$

where $N_1=0, 1, 2, \dots$. We can compare the master equation with the rate equation by deriving an equation for the first moment of $P(N_1)$ [44]. This is done by taking the time derivative of $\langle N_1 \rangle = \sum_{N_1} N_1 P(N_1)$, and inserting $\dot{P}(N_1)$ from Eq. (5). After performing the summation over the values of N_1 , one obtains the equation

$$\langle \dot{N}_1 \rangle = G_1 - D_1 \langle N_1 \rangle - 2K_{11} \langle N_1(N_1-1) \rangle, \quad (6)$$

which can be easily compared with Eq. (4).

The rate equation (4) and the master equation (5) include three rate constants: G_1 , D_1 and K_{11} . Therefore, their steady-state solutions, $\langle \dot{N}_1 \rangle = 0$ and $\dot{P}(N_1) = 0$, respectively, can be fully characterized by two parameters, which represent ratios between these three rates. We have chosen the ratios G_1/D_1 and D_1/K_{11} , the significance of which is as follows. The first parameter

$$S_{11}^+ = G_1/D_1, \quad (7)$$

represents the number of X_1 particles added to the system during the lifetime of one such particle. This value approximates the average number of potential reaction partners per X_1 particle. The second parameter

$$S_{11}^- = D_1/K_{11}, \quad (8)$$

is approximately the number of X_1 particles that degrade during the average time it takes an X_1 particle to undergo a reaction. These two parameters are used in order to characterize the dynamics of the system. If $S_{11}^+ > S_{11}^-$, the number of potential partners per particle is larger than the number that leave before it reacts. The range of parameters in which this situation occurs is called the reaction domain, since most

particles in the system undergo reaction rather than degradation. In the opposite situation, where $S_{11}^+ < S_{11}^-$, most particles leave the system through degradation before a reaction can take place. Thus, this range of parameters is called the degradation domain.

The rate equation method is expected to fail in the limit of small population sizes, where stochastic effects become significant. Naively, one may expect the rate equations to become inaccurate when $\langle N_1 \rangle < 1$. This is not a good criterion for several reasons. First, this condition cannot be easily evaluated in advance, based on the parameters alone: It requires one to actually solve the rate equations. Second, we will show below that it is possible to find a more accurate division between the deterministic and the stochastic regimes in the parameter space. Interestingly, it is found that in some cases the rate equations are applicable even for a range of parameters in which $\langle N_1 \rangle$ is significantly smaller than 1.

In order to characterize the stochastic range in a more precise manner, we compare the approximate results obtained from the rate equations with the exact results obtained from the master equation. More specifically, we use the analytical solution of the master equation (5), presented in Refs. [28,53]. In Fig. 1(a) we present the average population size $\langle N_1 \rangle$, obtained from the master equation under steady-state conditions, as a function of the parameters S_{11}^+ and S_{11}^- . The color code represents the function $y = \log_{10}(\langle N_1 \rangle)$. It is found that $\langle N_1 \rangle < 1$ (or $y < 0$) in a broad range of parameters covering the bottom half of the plot and the upper-left corner (dark shades). In Fig. 1(b) we compare the results for the reaction rate, R_{11} , obtained from the rate equation and the master equation, under steady-state conditions. The color code represents the function $z = \log_{10}(R_{11}^{\text{rate}}/R_{11}^{\text{master}})$. When the two results do not coincide, the rate equation is found to overestimate the reaction rate, namely $R_{11}^{\text{rate}} > R_{11}^{\text{master}}$, and $z > 0$. The rate equation provides a good approximation for R_{11} in the dark region, where $z \ll 1$, which is roughly characterized by

$$\max(S_{11}^+, S_{11}^-) > 1. \quad (9)$$

If the condition $\langle N_1 \rangle > 1$ was an accurate criterion for the validity of the rate equations, there would be no overlap between the dark region in Fig. 1(a) (where $\langle N_1 \rangle < 1$) and the dark region in Fig. 1(b) (where the rate equation results are valid). However, there is a large domain of such overlap in the lower-right quarter of the graph and a smaller one in the upper-left quarter. This indicates that the domain of validity of the rate equation is broader than expected.

The result presented in Eq. (9) can be intuitively understood as follows. In the reaction-dominated region [above the dashed line in Fig. 1(b)], most particles leave the system through reaction. In this case, the rate equation provides a good approximation for the reaction rate if the stochastic effects are small, namely if the average number of potential partners for reaction per particle is larger than 1 ($S_{11}^+ > 1$). In the degradation-dominated region [below the dashed line in Fig. 1(b)], the primary process is degradation. The rate equation solution and the master equation solution both converge toward $R_{11} \rightarrow 0$ as the degradation process becomes increasingly efficient. As can be seen by comparison of Eqs. (4) and

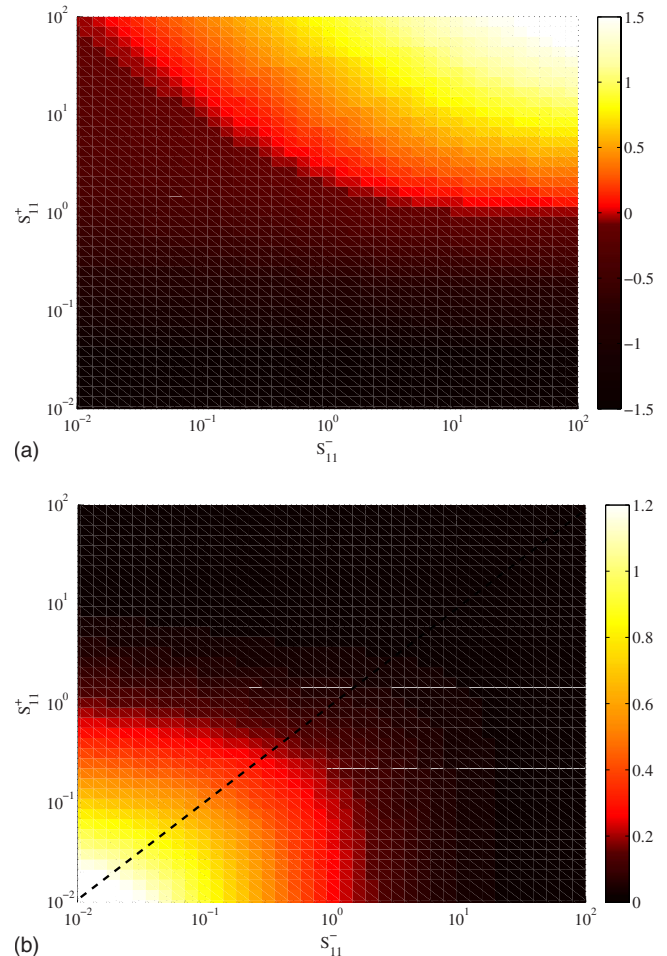


FIG. 1. (Color online) (a) The function $y = \log_{10}(\langle N_1 \rangle)$ in the steady state from the exact master equation solution vs the rate ratios $S_{11}^+ = G_1/D_1$ and $S_{11}^- = D_1/K_{11}$. The dark region represents the values for which $\langle N_1 \rangle < 1$. (b) The function $z = \log_{10}(R_{11}^{\text{rate}}/R_{11}^{\text{master}})$ vs S_{11}^+ and S_{11}^- under steady-state conditions. The dark region represents the values for which the rate equation method is accurate. This area can be roughly characterized as $\max(S_{11}^+, S_{11}^-) > 1$. The black dashed line separates the reaction domain (upper triangle) from the degradation domain (lower triangle).

(6), When the reaction rate becomes very low, the rate equation results coincide with those of the master equation. We can roughly characterize this region by $S_{11}^- > 1$.

III. SYSTEM-SIZE APPROACH

The steady state of the system described above is fully determined by the parameters $S_{11}^+ = G_1/D_1$ and $S_{11}^- = D_1/K_{11}$. This allows us to characterize the stochastic properties of this system through simple two-dimensional plots, such as those shown in Fig. 1. More complex networks involve too many parameters to allow such graphical analysis. Consequently, a different approach is required in order to formulate conditions similar to Eq. (9) for more general reaction networks. In order to find such conditions, we examine the dependence of the reaction rates on the system size Ω . Depending on the system being considered, the size Ω may refer to its volume,

area, or the number of discrete sites in which particles may reside. In general, we denote the units of Ω by $[\Omega]$ (which could represent, for example, cm^2 or cm^3 , depending on the system). In this analysis the rate constants are assumed to relate to Ω as follows. The generation rate G_i of species X_i is considered to be proportional to Ω according to

$$G_i = g_i \Omega, \quad (10)$$

where g_i ($\text{s}^{-1}[\Omega]^{-1}$) is a constant. An example of such a system is a surface exposed to a flux of particles. The reaction rate constant, K_{ij} , is taken to be inversely proportional to Ω , namely

$$K_{ij} = \frac{k_{ij}}{\Omega}. \quad (11)$$

where k_{ij} ($\text{s}^{-1}[\Omega]$) is a constant. This is the case, for example, in a system of particles which diffuse randomly on a surface and must encounter each other in order to react (a more precise evaluation of the reaction rate constant in the case of surface diffusion is given in Refs. [54,55]). The degradation rate D_i , which represents the inverse of the average lifetime of a single particle, is assumed to be independent of the system size. Therefore, the system can be fully described by the size-independent parameters g_i , k_{ij} , and D_i , and the system size Ω . It is important to note that these assumptions have been made for the sake of convenience and do not affect the final conclusions, which can be formulated in terms of the general parameters S_{ij}^{\pm} .

The rate equation method is based on the mean-field approximation, according to which the discrete particles can be replaced by a uniform density ρ_i of particles spread throughout the system. The average particle population is thus proportional to the system size,

$$\langle N \rangle = \rho_i \Omega. \quad (12)$$

Substituting $\rho_i \Omega$ for $\langle N \rangle$ in Eq. (1), we find that in the rate equation approach the reaction rate is also proportional to the system size

$$R_{ij} = \begin{cases} (k_{ii} \rho_i^2) \Omega & \text{for } i = j, \\ (k_{ij} \rho_i \rho_j) \Omega & \text{for } i \neq j. \end{cases} \quad (13)$$

In a large system, which contains many particles, the mean-field approximation is valid. However, as Ω is reduced (keeping the densities ρ_i constant), fluctuations in the number of particles become increasingly significant. Such conditions may also be reached by decreasing the densities ρ_i for a fixed system size. However, taking the system size as the control parameter is more convenient for our analysis. The effects of fluctuations are most straightforward when the system is small enough that $\langle N_i \rangle < 1$. Most of the time, such a system contains no more than one reactive particle, so no reaction can occur. However, the mean-field approximation attributes a nonzero reaction rate to the system. Generally, if the system is sufficiently small, the mean-field approximation will overestimate the reaction rate [20,21] and the actual reaction rate will no longer be proportional to Ω .

In the analysis below, we will try to identify the system size Ω above which the mean-field approximation is valid

and the rate equations are applicable. To this end, it is useful to consider the solution of the moment equations. These equations are constructed from the master equation, using a suitable truncation [44–46]. The moment equations are accurate for small systems in which the populations of reactive species are small. Depending on the network parameters, the moment equations may be valid for large systems as well [46].

The single-species system considered above can be described by the following set of moment equations [44];

$$\langle \dot{N}_1 \rangle = G_1 - D_1 \langle N_1 \rangle - 2K_{11}(\langle N_1^2 \rangle - \langle N_1 \rangle),$$

$$\langle \dot{N}_1^2 \rangle = G_1 + (2G_1 + D_1) \langle N_1 \rangle - 2D_1 \langle N_1^2 \rangle - 4K_{11}(\langle N_1^2 \rangle - \langle N_1 \rangle). \quad (14)$$

The reaction rate, $R_{11} = K_{11}(\langle N_1^2 \rangle - \langle N_1 \rangle)$, can be obtained by solving these two equations. In order to isolate the effect of the system size, we write the steady-state reaction rate, obtained from the moment equations, using the size-independent parameters [44,46],

$$R_{11}^{\text{moment}} = \frac{g_1^2}{D_1} \left(\frac{\Omega^2}{\alpha_{11}} \right), \quad (15)$$

where

$$\alpha_{11} = 1 + 2 \frac{\Omega}{(D_1/g_1)} + \frac{\Omega}{(k_{11}/D_1)}. \quad (16)$$

This expression reveals a dependence on two characteristic scales,

$$\begin{aligned} \Omega_{11}^+ &= \frac{D_1}{g_1} = \frac{\Omega}{S_{11}^+}, \\ \Omega_{11}^- &= \frac{k_{11}}{D_1} = \frac{\Omega}{S_{11}^-}, \end{aligned} \quad (17)$$

which represent the main features of the system, independently of the system size [53]. Thus, these scales serve as yardsticks for the evaluation of the system size. According to Eq. (16), the system size Ω is considered to be large if it is significantly larger than either Ω_{11}^+ or Ω_{11}^- . In a large system, α_{11} is proportional to Ω . Thus, according to Eq. (15), $R_{11}^{\text{moment}} \propto \Omega$. We can similarly conclude that if $\Omega < \min(\Omega_{11}^+, \Omega_{11}^-)$, the system is considered to be small. In this case, α_{11} is only weakly dependent on Ω and therefore $R_{11}^{\text{moment}} \propto \Omega^2$.

We now propose that this classification of large and small systems also applies as a criterion for the validity of the mean-field approximation. This leads to the conclusion that the condition for the use of the rate equations to evaluate the reaction rate is

$$\Omega > \min(\Omega_{11}^+, \Omega_{11}^-). \quad (18)$$

This condition is identical to Eq. (9), which was found empirically from Fig. 1. This result is illustrated by two examples in Fig. 2. In these examples, the steady-state reaction rate is shown as a function of the system size Ω . The Ω axis

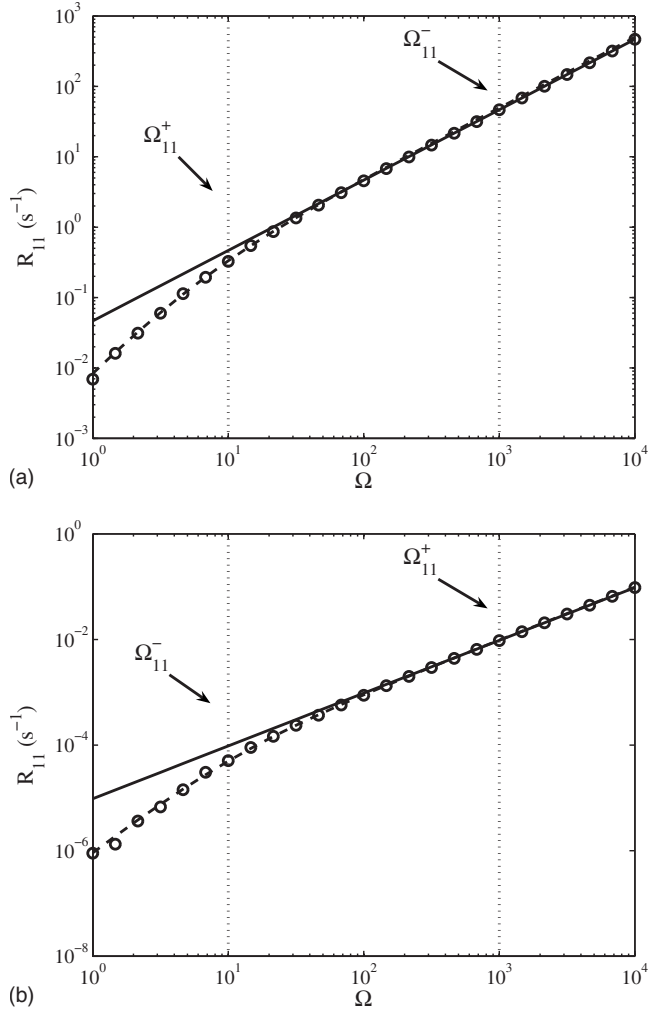


FIG. 2. The reaction rate R_{11} vs system size Ω for the reaction $X_1 + X_1 \rightarrow X_2$, under steady-state conditions. The solution of the rate equation (solid line) is compared with the results of the stochastic simulation (circles). The solution of the moment equations (dashed line) appears as well. Examples from both the reaction domain $\Omega_{11}^+ < \Omega_{11}^-$ (a) and the degradation domain $\Omega_{11}^+ > \Omega_{11}^-$ (b) are presented. These results demonstrate that the solution of the rate equations accurately approximates the exact solution if $\Omega > \min(\Omega_{11}^+, \Omega_{11}^-)$.

in each of these plots corresponds to a diagonal line in the plane of Fig. 1. The rate equation results (solid line) are compared to the stochastic results, obtained from Monte Carlo simulations (circles). The moment equation results are also shown (dashed line) for comparison. In addition, the characteristic scales Ω_{11}^+ and Ω_{11}^- appear as vertical dotted lines. In each of the two examples, the rate equation results are accurate in the region $\Omega > \min(\Omega_{11}^+, \Omega_{11}^-)$. When Ω approaches the smaller of the two characteristic scales the actual reaction rate obtained from the stochastic methods ceases to be proportional to Ω and the rate equation results are not valid. This is in agreement with Eq. (18). In Fig. 2(a) the system is in the reaction domain, namely $\Omega_{11}^+ < \Omega_{11}^-$. In Fig. 2(b) the system is in the degradation domain, where $\Omega_{11}^+ > \Omega_{11}^-$.

The Monte Carlo results presented throughout this paper were obtained using the Gillespie algorithm [32,33]. The simulation is set in the space spanned by the discrete states of the system, corresponding to the values N_i , $i=1, \dots, n$. The simulation consists of a generalized random walk between states which are connected by different processes, weighted by their rates. The Monte Carlo data provides the probability of the system to be in each state. The average values obtained from this data converge towards the exact stochastic solution given by the master equation.

IV. GENERALIZATION TO MORE COMPLEX NETWORKS

We now extend the analysis of the preceding section to more complex reaction networks. As a first step, we consider a simple system involving two reactive species X_1 and X_2 . Particles of species X_i , $i=1, 2$, are added to the system at a constant rate G_i (s^{-1}), and undergo degradation at a rate D_i (s^{-1}). In addition, two particles may react according to $X_1 + X_2 \rightarrow X_3$ with a rate constant K_{12} (s^{-1}). For simplicity, we assume that the product species X_3 is not reactive and has no further role in the evolution of the system. Under these assumptions, the rate equations take the form

$$\begin{aligned} \langle \dot{N}_1 \rangle &= G_1 - D_1 \langle N_1 \rangle - K_{12} \langle N_1 \rangle \langle N_2 \rangle, \\ \langle \dot{N}_2 \rangle &= G_2 - D_2 \langle N_2 \rangle - K_{12} \langle N_1 \rangle \langle N_2 \rangle. \end{aligned} \quad (19)$$

To extend the system-size analysis, we define two parameters for each of the reactive species, which provide the ratios between the rates of different processes,

$$\begin{aligned} X_1 &\rightarrow \begin{cases} S_{12}^+ = G_2/D_1, \\ S_{12}^- = D_2/K_{12}, \end{cases} \\ X_2 &\rightarrow \begin{cases} S_{21}^+ = G_1/D_2, \\ S_{21}^- = D_1/K_{12}. \end{cases} \end{aligned} \quad (20)$$

The parameter S_{ij}^+ represents the number of potential reaction partners of type X_j per X_i particle. The parameter S_{ij}^- represents the number of X_j particles that leave the system in the average time it takes an X_i particle to undergo a reaction. Therefore, if $S_{ij}^+ > S_{ij}^-$ then the removal of particles of species X_i from the system is dominated by the reaction process rather than by degradation. In the opposite case, $S_{ij}^+ < S_{ij}^-$, the removal of X_i particles is dominated by degradation.

Implementing the system-size approach, we use the solution of the moment equations to identify the domain in which the rate equations accurately approximate the reaction rate. The moment equations for this system are [46]

$$\begin{aligned} \langle \dot{N}_1 \rangle &= G_1 - D_1 \langle N_1 \rangle - K_{12} \langle N_1 N_2 \rangle, \\ \langle \dot{N}_2 \rangle &= G_2 - D_2 \langle N_2 \rangle - K_{12} \langle N_1 N_2 \rangle, \end{aligned}$$

$$\langle N_1 \dot{N}_2 \rangle = G_1 \langle N_2 \rangle + G_2 \langle N_1 \rangle - (D_1 + D_2 + K_{12}) \langle N_1 N_2 \rangle. \quad (21)$$

Expressing the steady-state reaction rate, obtained from the solution of these equations, in terms of the size-independent

parameters, g_1, g_2, D_1, D_2 and $k_{12} = K_{12}/\Omega$, and the system size Ω , we find that

$$R_{12}^{\text{moment}} = g_1 g_2 \left(\frac{1}{D_1} + \frac{1}{D_2} \right) \left(\frac{\Omega^2}{\alpha_{12}} \right), \quad (22)$$

where

$$\alpha_{12} = 1 + \frac{\Omega}{(D_1/g_2)} + \frac{\Omega}{(D_2/g_1)} + \frac{\Omega}{(k_{12}/D_2)} + \frac{\Omega}{(k_{12}/D_1)}. \quad (23)$$

The dependence of R_{12}^{moment} in Eq. (22) on the system size appears only in the ratio Ω^2/α_{12} . This dependence is determined by the four characteristic scales, which appear in Eq. (23), namely $\Omega_{12}^+ = \Omega/S_{12}^+$, $\Omega_{21}^+ = \Omega/S_{21}^+$, $\Omega_{12}^- = \Omega/S_{12}^-$, and $\Omega_{21}^- = \Omega/S_{21}^-$. According to our hypothesis that the rate equations are accurate when $R_{12}^{\text{moment}} \propto \Omega$, the condition for the validity of the rate equations is

$$\Omega > \min(\Omega_{12}^+, \Omega_{12}^-, \Omega_{21}^+, \Omega_{21}^-). \quad (24)$$

This condition is demonstrated in Fig. 3. In Fig. 3(a) both species are in the reaction domain, namely $\Omega_{ij}^+ < \Omega_{ij}^-$. In Fig. 3(b) both species are in the degradation domain, namely $\Omega_{ij}^+ > \Omega_{ij}^-$. In both examples, the rate equations become inaccurate as Ω approaches the smallest of the four scales Ω_{12}^+ , Ω_{12}^- , Ω_{21}^+ , and Ω_{21}^- .

A. Networks with multiple reactions

Both systems considered thus far involve a single reaction. In order to generalize our analysis to more complex networks, we must examine a system with more than one reaction. Thus, we consider a system of three species X_1, X_2 , and X_3 , with two reactions $X_1 + X_2 \rightarrow X_4$ and $X_1 + X_3 \rightarrow X_5$. The rate equations that describe this system are

$$\begin{aligned} \langle \dot{N}_1 \rangle &= G_1 - D_1 \langle N_1 \rangle - K_{12} \langle N_1 \rangle \langle N_2 \rangle - K_{13} \langle N_1 \rangle \langle N_3 \rangle, \\ \langle \dot{N}_2 \rangle &= G_2 - D_2 \langle N_2 \rangle - K_{12} \langle N_1 \rangle \langle N_2 \rangle, \\ \langle \dot{N}_3 \rangle &= G_3 - D_3 \langle N_3 \rangle - K_{13} \langle N_1 \rangle \langle N_3 \rangle. \end{aligned} \quad (25)$$

In the simpler systems described above the kinetic behavior of each species was determined by the comparison of the reaction rate and the degradation rate of that species. When a certain species takes part in more than a single reaction, one needs to separately compare its degradation rate with the reaction rate of each of these reactions. Since each reaction involves two species, it is characterized by four rate-ratio parameters of the form

$$\begin{aligned} R_{12} &\rightarrow \begin{cases} S_{12}^+, S_{12}^- & \text{for } X_1, \\ S_{21}^+, S_{21}^- & \text{for } X_2, \end{cases} \\ R_{13} &\rightarrow \begin{cases} S_{13}^+, S_{13}^- & \text{for } X_1, \\ S_{31}^+, S_{31}^- & \text{for } X_3. \end{cases} \end{aligned} \quad (26)$$

The comparison between the parameters S_{ij}^+ and S_{ij}^- determines the relative strengths of the reaction R_{ij} and the deg-

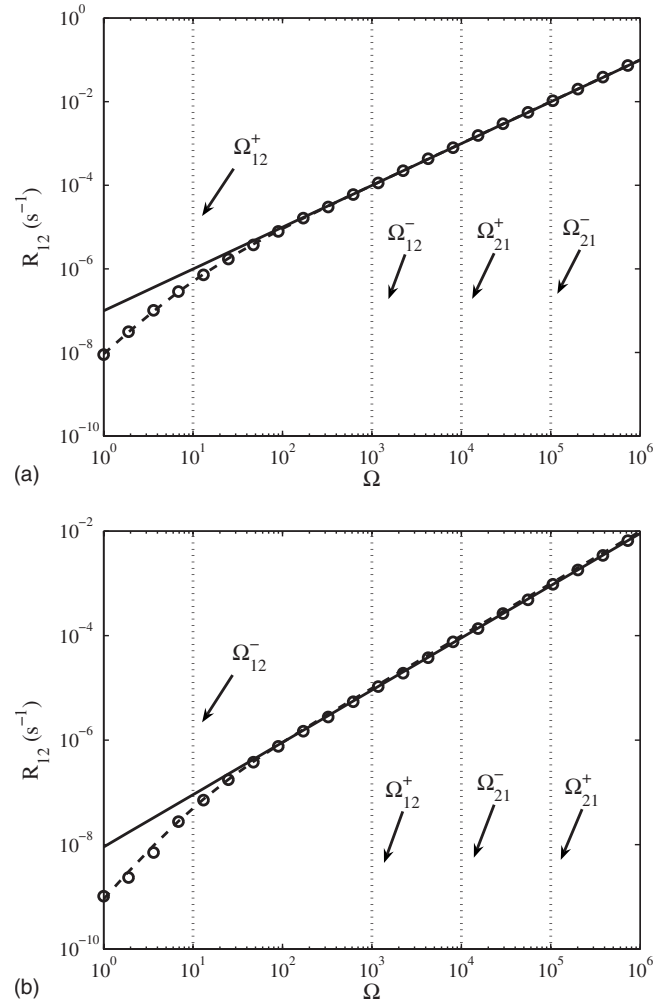


FIG. 3. The reaction rate R_{12} vs system size Ω for the two-species reaction network, under steady-state conditions. The solution of the rate equation (solid line), stochastic simulation (circles), and the moment equations (dashed line) are shown. In example (a) both species are in the reaction domain, and in (b) both are in the degradation domain. Both examples demonstrate that the rate equations are accurate when $\Omega > \min(\Omega_{12}^+, \Omega_{12}^-, \Omega_{21}^+, \Omega_{21}^-)$ and the actual reaction rate is proportional to Ω .

radation of the species X_i . For instance, if $S_{12}^+ > S_{12}^-$, the X_1 species has a stronger tendency to react with X_2 than to degrade. This is independent of the strength of the reaction of X_1 with X_3 , which is determined by S_{13}^+ and S_{13}^- , or the strength of $X_1 + X_2$ with regard to X_2 , which is determined by S_{21}^+ and S_{21}^- .

Employing the system-size approach, we are interested in the steady-state solution of the moment equations for this system, which take the form [46]

$$\begin{aligned} \langle \dot{N}_1 \rangle &= G_1 - D_1 \langle N_1 \rangle - K_{12} \langle N_1 N_2 \rangle - K_{13} \langle N_1 N_3 \rangle, \\ \langle \dot{N}_2 \rangle &= G_2 - D_2 \langle N_2 \rangle - K_{12} \langle N_1 N_2 \rangle, \\ \langle \dot{N}_3 \rangle &= G_3 - D_3 \langle N_3 \rangle - K_{13} \langle N_1 N_3 \rangle, \end{aligned}$$

$$\langle \dot{N}_1 \dot{N}_2 \rangle = G_1 \langle N_2 \rangle + G_2 \langle N_1 \rangle - (D_1 + D_2 + K_{12}) \langle N_1 N_2 \rangle,$$

$$\langle \dot{N}_1 \dot{N}_3 \rangle = G_1 \langle N_3 \rangle + G_3 \langle N_1 \rangle - (D_1 + D_3 + K_{13}) \langle N_1 N_3 \rangle. \quad (27)$$

In this case, it is not possible to derive simple expressions for the steady-state reaction rates from these moment equations. However, under steady-state conditions it is possible to express the reaction rate $R_{12} = K_{12} \langle N_1 N_2 \rangle$ in terms of $R_{13} = K_{13} \langle N_1 N_3 \rangle$, according to

$$R_{12}^{\text{moment}} = g_1 g_2 \left[\frac{1}{D_1} \left(1 - \frac{r_{13}^{\text{moment}}}{g_1} \right) + \frac{1}{D_2} \right] \left(\frac{\Omega^2}{\alpha_{12}} \right), \quad (28)$$

where $r_{13} = R_{13}/\Omega$. Note that the expression for R_{13}^{moment} can be obtained in a similar fashion. Equation (28) is similar in form to Eq. (22), except for the term $r_{13}^{\text{moment}}/g_1$. In systems which involve only one reaction, the dependence of the steady-state reaction rate R_{ij}^{moment} on the system size is entirely determined by the ratio Ω^2/α_{ij} . However, the inclusion of a second reaction $X_i + X_k$ adds a dependence on r_{ik}^{moment} , which, in general, may be dependent on Ω . The analysis is further complicated by the fact that the moment equations may become inaccurate in the large Ω limit as the reaction network becomes more complex.

The central factor in evaluating the system-size dependence in Eq. (28) is the importance of the term $r_{13}^{\text{moment}}/g_1$. If most X_1 particles react with particles of species X_3 , then $r_{13}^{\text{moment}}/g_1 \rightarrow 1$, and its dependence on Ω may have a large influence on R_{12}^{moment} . On the other hand, if other processes dominate the X_1 population, then $r_{13}^{\text{moment}}/g_1 \ll 1$, and can be neglected. The strength of the reaction process can be roughly estimated according to the ratio $\Omega_{13}^-/\Omega_{13}^+$. If $\Omega_{13}^-/\Omega_{13}^+ \ll 1$, only a minority of the X_1 particles are able to find an X_3 particle to react with. Therefore, the value of $r_{13}^{\text{moment}}/g_1$ is small. In the opposite case, $\Omega_{13}^-/\Omega_{13}^+ \gg 1$, the X_1 particles have ample opportunity to react with X_3 particles. However, if $\Omega_{12}^-/\Omega_{12}^+ > \Omega_{13}^-/\Omega_{13}^+$, many X_1 particles will react with X_2 particles instead, thus reducing the value of $r_{13}^{\text{moment}}/g_1$. The limit $r_{13}^{\text{moment}}/g_1 \rightarrow 1$ may be reached if $\Omega_{13}^-/\Omega_{13}^+ \gg 1$, and $\Omega_{12}^-/\Omega_{12}^+ < \Omega_{13}^-/\Omega_{13}^+$.

When the X_1 species is largely dominated by degradation, namely, $\Omega_{1j}^-/\Omega_{1j}^+ \ll 1$ for $j=2,3$, the coupling between the two reactions is reduced and the analysis of the system can be simplified. In this case, r_{12} and r_{13} are both much smaller than g_1 and their dependence on the system size does not affect the reaction rates. Consequently, Eq. (28) is effectively reduced to the expression (22) for the reaction rate in a two-species system. Therefore, the dependence of each rate R_{ij}^{moment} in the three-species system on Ω is determined in the same manner as the single rate in the two-species system. Defining

$$\Omega_{ij}^{\text{min}} = \min(\Omega_{ij}^+, \Omega_{ij}^-, \Omega_{ji}^+, \Omega_{ji}^-), \quad (29)$$

we conclude that the rate equations may be used for the calculation of R_{ij} as long as the system size satisfies

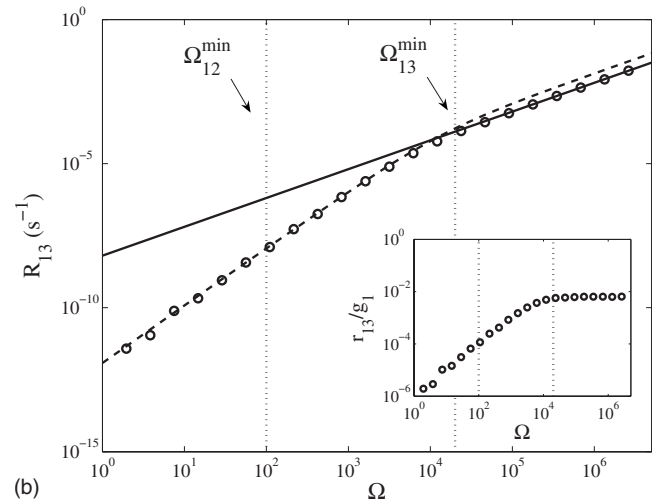
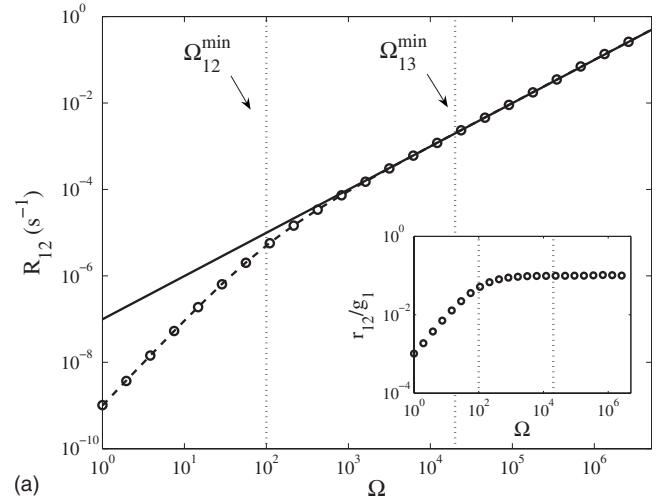


FIG. 4. Steady-state reaction rates (a) R_{12} and (b) R_{13} vs system size Ω in the three species reaction network. The solution of the rate equation (solid line), stochastic simulation (circles), and the moment equations (dashed line) are shown. The inset plots show the ratios (a) r_{12}/g_1 and (b) r_{13}/g_1 , which are both significantly smaller than 1. Therefore, the rate equations provide an accurate approximation of each rate R_{ij} if the condition $\Omega > \Omega_{ij}^{\text{min}}$ is fulfilled.

$$\Omega > \Omega_{ij}^{\text{min}}. \quad (30)$$

An example of such a system, where $\Omega_{12}^-/\Omega_{12}^+ = 10$ and $\Omega_{13}^-/\Omega_{13}^+ = 0.02$ is shown in Fig. 4. The steady-state value of R_{12} versus Ω is shown in Fig. 4(a). As in the two species system, the rate equation results for R_{12} are valid as long as $\Omega > \Omega_{12}^{\text{min}}$. The inset shows the value of r_{12}/g_1 vs Ω , which is smaller than 1 by at least an order of magnitude. It is clear from Fig. 4(b) that the crossover to the stochastic regime with respect to R_{13} takes place at $\Omega = \Omega_{13}^{\text{min}}$. The inset shows the ratio r_{13}/g_1 , which is much smaller than 1.

When the X_1 population is dominated by one or more reactions, it becomes more difficult to identify the boundary of the stochastic domain for each reaction separately. This is due to the fact that the system size dependence of R_{12} , given by Eq. (28), may be influenced by the term $r_{13}^{\text{moment}}/g_1$. Even a relatively simple network, such as this three species sys-

tem, involves too many factors to accurately determine the point at which the rate equation solution begins to deviate from the exact solution. However, we can find an upper bound for this point. To this end we employ several assumptions regarding the behavior of the system in two limits.

According to our analysis of simpler systems, the entire system is in the stochastic limit when

$$R_{ij}^{\text{moment}} \propto \Omega^2 \quad (31)$$

for both reactions. This is the case if

$$\Omega < \min(\Omega_{12}^{\min}, \Omega_{13}^{\min}), \quad (32)$$

since most particles leave the system by degradation before they have a chance to undergo reaction. Therefore, both r_{12} and r_{13} are much smaller than g_1 , and can be neglected. Furthermore, under the condition of Eq. (32), both parameters α_{12} and α_{13} are ≈ 1 [see Eq. (23)]. As apparent from Eq. (28), this means that both R_{12} and R_{13} are in the stochastic limit.

For large systems we assume that fluctuations in the particle populations are negligible. Therefore, it is generally assumed that the rate equations are accurate in the large system limit, although this limit is usually determined rather heuristically. Based on the system-size approach, we consider the system to be large if Ω is larger than the minimal scales associated with both reactions,

$$\Omega > \max(\Omega_{12}^{\min}, \Omega_{13}^{\min}). \quad (33)$$

This also corresponds to the domain in which, for both reactions,

$$R_{ij}^{\text{moment}} \propto \Omega, \quad (34)$$

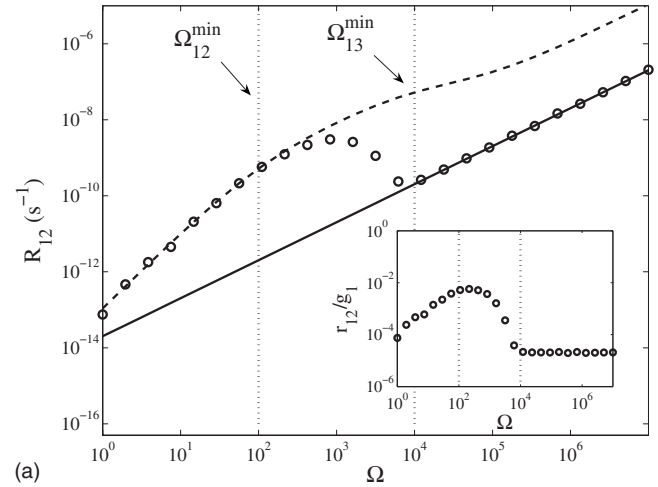
although the solution of the moment equations may not be accurate in this limit. In this domain, the deterministic mean-field approximation is valid for both reactions, and the rate equations may be used to calculate both reaction rates.

These assumptions are justified regardless of which process dominates the population size of each particle species. As we have seen, if both reactions are relatively inefficient, neither has a significant effect on the other. Therefore, we are able to separately pinpoint the transition of each reaction rate R_{ij} from deterministic to stochastic behavior as Ω_{ij}^{\min} . In the event that at least one reaction is very effective with regard to the X_1 species, the reaction rates are influenced by one another. Based on our conclusion that the rate equations are accurate for both reaction rates if

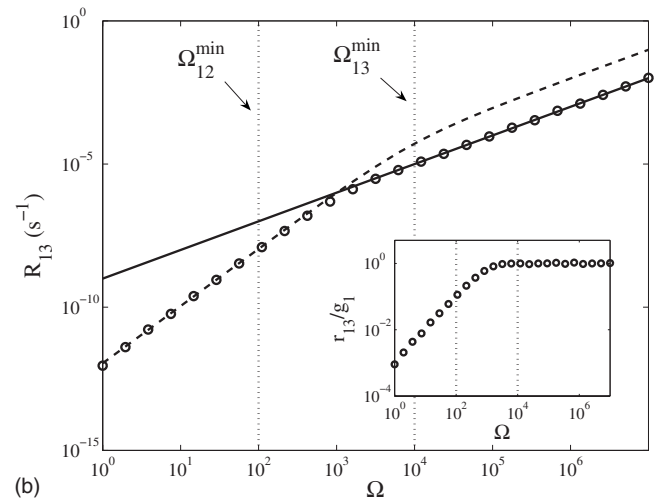
$$\Omega > \max(\Omega_{12}^{\min}, \Omega_{13}^{\min}), \quad (35)$$

and without performing a more complex analysis, the most we can say about either reaction rate is that the transition occurs somewhere between the two scales Ω_{12}^{\min} and Ω_{13}^{\min} . We can thus set the upper bound for the transition point for both reaction rates to be $\max(\Omega_{12}^{\min}, \Omega_{13}^{\min})$.

In the example presented in Fig. 5, the parameter ratios are $\Omega_{12}^-/\Omega_{12}^+ = 0.01$ and $\Omega_{13}^-/\Omega_{13}^+ = 500$. Accordingly, $r_{12}/g_1 \ll 1$, as can be seen in the inset of Fig. 5(a), and $r_{13}/g_1 \rightarrow 1$ in the large system limit, as is apparent from the inset of Fig. 5(b). The results obtained from Monte Carlo simulations,



(a)



(b)

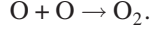
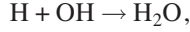
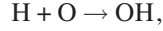
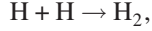
FIG. 5. Steady-state reaction rates (a) R_{12} and (b) R_{13} vs system size Ω in the three species reaction network. The solution of the rate equation (solid line), stochastic simulation (circles), and the moment equations (dashed line) are shown. The inset plots show the ratios (a) r_{12}/g_1 and (b) r_{13}/g_1 , which approaches 1 in the large system limit. If $\Omega < \min(\Omega_{12}^{\min}, \Omega_{13}^{\min})$, both reactions are in the stochastic domain, $R_{ij} \propto \Omega^2$ ($r_{ij} \propto \Omega$). If $\Omega > \max(\Omega_{12}^{\min}, \Omega_{13}^{\min})$, the mean-field approximation is valid for both reactions and $R_{ij} \propto \Omega$ ($r_{ij} \sim \text{const}$). In this domain, the rate equations provide an accurate approximation of both rates R_{12} and R_{13} .

indicate that in the limit $\Omega < \min(\Omega_{12}^{\min}, \Omega_{13}^{\min}) = 10^2$ both reactions are in the stochastic domain, where $R_{ij} \propto \Omega^2$ ($r_{ij} \propto \Omega$). When $\Omega > \max(\Omega_{12}^{\min}, \Omega_{13}^{\min}) = 10^4$, the mean-field approximation is valid for both reactions and $R_{ij} \propto \Omega$. In this domain, the rate equations provide an accurate approximation of both rates R_{12} and R_{13} .

B. Example: Formation of water molecules on surfaces

In a general reaction network, each reactive species may participate in several reactions. Additionally, particles which are products of one reaction may react with other species. These features may complicate the equations that describe such reaction networks. However, the same principles we have used in the analysis of the simpler networks apply in

the general case as well. As an example, we consider the following set of chemical reactions:



This network is of much interest in interstellar chemistry. It takes part in the formation of ice mantles on the surfaces of dust grains in dense molecular clouds in the galaxy [56,57]. Each reaction process is associated with its own set of parameters,

$$R_{ij} \rightarrow \begin{cases} \Omega_{ii}^+, \Omega_{ii}^- & \text{for } i=j, \\ \Omega_{ij}^+, \Omega_{ij}^-, \Omega_{ji}^+, \Omega_{ji}^- & \text{for } i \neq j, \end{cases} \quad (36)$$

making a total of 12 parameters for this network. Following the system-size approach, we are interested in the steady-state solution of the moment equations for each of the reaction rates R_{ij} . Our system is described by a set of seven moment equations [46],

$$\langle \dot{N}_H \rangle = G_H - D_H \langle N_H \rangle - 2R_{H,H} - R_{H,O} - R_{H,OH},$$

$$\langle \dot{N}_O \rangle = G_O - D_O \langle N_O \rangle - 2R_{O,O} - R_{H,O},$$

$$\langle \dot{N}_{OH} \rangle = G_{OH} - D_{OH} \langle N_{OH} \rangle + R_{H,O} - R_{H,OH},$$

$$\langle \dot{N}_H^2 \rangle = G_H + (2G_H + D_H) \langle N_H \rangle - 2D_H \langle N_H^2 \rangle - 4R_{H,H} - R_{H,O} - R_{H,OH},$$

$$\langle \dot{N}_O^2 \rangle = G_O + (2G_O + D_O) \langle N_O \rangle - 2D_O \langle N_O^2 \rangle - 4R_{O,O} - R_{H,O},$$

$$\langle \dot{N}_H N_O \rangle = G_H \langle N_O \rangle + G_O \langle N_H \rangle - (D_H + D_O + K_{H,O}) \langle N_H N_O \rangle,$$

$$\langle \dot{N}_H N_{OH} \rangle = G_H \langle N_{OH} \rangle + G_{OH} \langle N_H \rangle - (D_H + D_{OH} + K_{H,OH}) \langle N_H N_{OH} \rangle. \quad (37)$$

For simplicity, we have represented terms of the form $K_{ii}(\langle N_i^2 \rangle - \langle N_i \rangle)$ by R_{ii} and terms of the form $K_{ij}\langle N_i N_j \rangle$ by R_{ij} .

As in the previous system, it is possible to find simple expressions for the reaction rates if, while solving for R_{ij} we treat all other reaction rates as constants. Using the parameters g , D , k , and r , we find that the reaction rates in this system are

$$R_{H,H} = g_H^2 \left[\frac{1}{D_H} \left(1 - \frac{r_{H,O} + r_{H,OH}}{g_H} \right) \right] \left(\frac{\Omega^2}{\alpha_{H,H}} \right), \quad (38)$$

$$R_{O,O} = g_O^2 \left[\frac{1}{D_O} \left(1 - \frac{r_{H,O}}{g_O} \right) \right] \left(\frac{\Omega^2}{\alpha_{O,O}} \right), \quad (39)$$

$$R_{H,O} = g_H g_O \left[\frac{1}{D_H} \left(1 - \frac{2r_{H,H} + r_{H,OH}}{g_H} \right) + \frac{1}{D_O} \left(1 - \frac{2r_{O,O}}{g_O} \right) \right] \times \left(\frac{\Omega^2}{\alpha_{H,O}} \right), \quad (40)$$

$$R_{H,OH} = g_H g_{OH} \left[\frac{1}{D_H} \left(1 - \frac{2r_{H,H} + r_{H,O}}{g_H} \right) + \frac{1}{D_{OH}} \left(1 + \frac{r_{H,O}}{g_{OH}} \right) \right] \times \left(\frac{\Omega^2}{\alpha_{H,OH}} \right). \quad (41)$$

The parameters α_{ii} and α_{ij} are given by Eqs. (16) and (23), respectively. Expressions (38)–(41) are similar to the ones derived for the simpler systems. In a similar manner, we can obtain the steady-state expressions for the reaction rates in any system of reacting particles. The values of the competition terms relative to 1 determine the system-size dependence of the reaction rates. However, as the reaction network becomes more complex, it becomes increasingly difficult to estimate these values based on the system parameters alone. For a general system, therefore, we can find only an upper limit for the transition value of the system size by applying the conclusions of the preceding sections. To calculate a particular rate R_{ij} , we must compare the system size to Ω^{\min} for all the reactions which involve either X_i or X_j . If Ω is smaller than all of them, then R_{ij} is in the stochastic limit, where $R_{ij} \propto \Omega^2$. If Ω is larger than all the Ω^{\min} associated with X_i and X_j , the mean-field approximation is valid and the rate equations may be used to calculate R_{ij} . Thus, for instance, the rate equation solution for $R_{O,O}$ will be accurate if $\Omega > \max(\Omega_{O,O}^{\min}, \Omega_{H,O}^{\min})$, and for $R_{H,OH}$ if $\Omega > \max(\Omega_{H,H}^{\min}, \Omega_{H,O}^{\min}, \Omega_{H,OH}^{\min})$.

V. SUMMARY AND DISCUSSION

Reaction networks exhibit deterministic behavior for large systems in which the populations of reactive species are large and fluctuations are negligible. In this case they can be simulated using rate equations. In the limit of small systems, the populations of reactive species are small and their discrete nature becomes important. Therefore, fluctuations are significant and stochastic methods are required for the simulation of these systems.

In this paper we have addressed the problem of identifying the conditions under which the rate equations may be used to calculate reaction rates in a general system. This question is important since the rate equations are much more efficient in terms of computational resources than stochastic methods. More specifically, the rate equations include one equation for each reactive species. In the master equation, the number of equations increases exponentially with the number of species. To demonstrate this fact, consider a reaction network which includes n reactive species, X_i , $i = 1, \dots, n$. The master equation accounts for the time derivatives of the probabilities $P(N_1, N_2, \dots, N_n)$ that the population sizes of species X_i , $i = 1, \dots, n$, will be given by N_i . In numerical simulations the master equation must be truncated in order to keep the number of equations finite. This is done

by setting upper cutoffs N_i^{\max} , $i=1, \dots, n$ on the population sizes such that $N_i=0, 1, \dots, N_i^{\max}$. The number of equations is thus $N_E = \prod_{i=1}^n (N_i^{\max} + 1)$. The truncated master equation is valid as long as the probability to have population sizes beyond the cutoffs is vanishingly small. Clearly, N_E grows exponentially with n . This severely limits the applicability of the master equation. Similarly, the time required for Monte Carlo simulations to converge is proportional to the volume of the relevant state space, which increases exponentially with the number of species. Several methods which combine both stochastic and deterministic calculations have recently been developed in order to maximize both the efficiency and accuracy of the simulation. In Ref. [50] this problem is addressed by using an adaptive stochastic method, that dynamically switches between deterministic and stochastic simulations according to the population sizes of the reactive species and the reaction rate constant. References [48,49] introduce methods in which a reaction network is partitioned into fast reactions and slow reactions. The fast reactions, in which fluctuations are negligible, are integrated using deterministic equations (or Langevin equations), while the slow reactions are simulated using stochastic methods. Both these approaches rely on intuitive criteria for identifying the reactions which require the use of stochastic calculations. Additionally, the methods of Refs. [50,49] require reevaluation of the need for stochastic calculations at every step of the simulation.

We have used the system size approach to formulate well-defined criteria for the crossover from deterministic to stochastic behavior in networks of chemical reactions. In our analysis it is assumed that the reactants are distributed homogeneously in space or are constantly stirred. Using this

approach we identified the range of conditions under which the rate equations provide accurate results for the reaction rates in the network. These conditions are expressed in terms of the rate constants of the network. They can thus be evaluated prior to the actual execution of the simulation. Therefore, these conditions enable one to choose the proper simulation method for the given network.

For simple systems involving a single reaction, we identify several characteristic scales defined by the rate constants of the system. The system is found to exhibit deterministic behavior as long as its size is larger than the smallest of these scales. In more complex networks, each species may participate in more than one reaction. Each of these reactions is associated with several characteristic scales. However, the deterministic regime for a given reaction is not fully defined by these scales alone, rather the effects of competing reactions must be taken into account as well. In general, these effects cannot be evaluated *a priori* from the system parameters, since they depend on the relative efficiency of the different reactions. For a given reaction in a general network, we can only identify an upper bound for the system size at which the crossover between deterministic and stochastic behavior takes place. As long as the system is larger than this upper bound, the rate equations are suitable for the calculation of the rate of this reaction.

ACKNOWLEDGMENTS

We thank Baruch Barzel for helpful discussions. This work was supported by the Israel Science Foundation, the Adler Foundation for Space Research and the US-Israel Binational Science Foundation.

-
- [1] K. A. Connors, *Chemical Kinetics: The Study of Reaction Rates in Solution* (Wiley, New York, 1990).
 - [2] J. D. Murray, *Mathematical Biology* (Springer, Berlin, 1989).
 - [3] Yu. Suchorski, R. Imbihl, and V. K. Medvedev, *Surf. Sci.* **401**, 392 (1998).
 - [4] Yu. Suchorski, J. Beben, E. W. James, J. W. Evans, and R. Imbihl, *Phys. Rev. Lett.* **82**, 1907 (1999).
 - [5] Yu. Suchorski, J. Beben, R. Imbihl, E. W. James, D.-J. Liu, and J. W. Evans, *Phys. Rev. B* **63**, 165417 (2001).
 - [6] V. Johaneck, M. Laurin, A. W. Grant, B. Kasemo, C. R. Henry, and J. Libuda, *Science* **304**, 1639 (2004).
 - [7] M. Pineda, R. Imbihl, L. Schimansky-Geier, and Ch. Züllicke, *J. Chem. Phys.* **124**, 044701 (2006).
 - [8] D.-J. Liu and J. W. Evans, *J. Chem. Phys.* **117**, 7319 (2002).
 - [9] L. Spitzer, *Physical Processes in the Interstellar Medium* (Wiley, New York, 1978).
 - [10] T. W. Hartquist and D. A. Williams, *The Chemically Controlled Cosmos* (Cambridge University Press, Cambridge, UK, 1995).
 - [11] A. G. G. M. Tielens, *The Physics and Chemistry of the Interstellar Medium* (Cambridge University Press, Cambridge, UK, 2005).
 - [12] T. I. Hasegawa, E. Herbst, and C. M. Leung, *Astrophys. J., Suppl. Ser.* **82**, 167 (1992).
 - [13] E. Herbst, *Annu. Rev. Phys. Chem.* **46**, 27 (1995).
 - [14] R. J. Gould and E. E. Salpeter, *Astrophys. J.* **138**, 393 (1963).
 - [15] D. Hollenbach and E. E. Salpeter, *J. Chem. Phys.* **53**, 79 (1970).
 - [16] D. Hollenbach and E. E. Salpeter, *Astrophys. J.* **163**, 155 (1971).
 - [17] D. Hollenbach, M. W. Werner, and E. E. Salpeter, *Astrophys. J.* **163**, 165 (1971).
 - [18] A. G. G. M. Tielens and W. Hagen, *Astron. Astrophys.* **114**, 245 (1982).
 - [19] S. B. Charnley, A. G. G. M. Tielens, and S. D. Rodgers, *Astrophys. J.* **482**, L203 (1997).
 - [20] P. Caselli, T. I. Hasegawa, and E. Herbst, *Astrophys. J.* **495**, 309 (1998).
 - [21] O. M. Shalabiea, P. Caselli, and E. Herbst, *Astrophys. J.* **502**, 652 (1998).
 - [22] H. H. McAdams and A. Arkin, *Proc. Natl. Acad. Sci. U.S.A.* **94**, 814 (1997).
 - [23] A. Arkin, J. Ross, and H. H. McAdams, *Genetics* **149**, 1633 (1998).
 - [24] J. Paulsson, *Nature (London)* **427**, 415 (2004).
 - [25] M. B. Elowitz, A. J. Levine, E. D. Siggia, and P. S. Swain, *Science* **297**, 1183 (2002).
 - [26] E. M. Ozbudak, M. Thattai, I. Kurtser, A. D. Grossman, and A.

- van Oudenaarden, *Nat. Genet.* **31**, 69 (2002).
- [27] O. Biham, I. Furman, V. Pirronello, and G. Vidali, *Astrophys. J.* **553**, 595 (2001).
- [28] N. J. B. Green, T. Toniazzo, M. J. Pilling, D. P. Ruffe, N. Bell, and T. W. Hartquist, *Astron. Astrophys.* **375**, 1111 (2001).
- [29] N. G. van Kampen, *Stochastic Processes in Physics and Chemistry* (North-Holland, Amsterdam, 1981).
- [30] C. W. Gardiner, *Handbook of Stochastic Methods* (Springer, Berlin, 2004).
- [31] J. Paulsson and M. Ehrenberg, *Phys. Rev. Lett.* **84**, 5447 (2000).
- [32] D. T. Gillespie, *J. Comput. Phys.* **22**, 403 (1976).
- [33] D. T. Gillespie, *J. Phys. Chem.* **81**, 2340 (1977).
- [34] M. E. J. Newman and G. T. Barkema, *Monte Carlo Methods in Statistical Physics* (Clarendon, Oxford, 1999).
- [35] S. B. Charnley, *Astrophys. J.* **562**, L99 (2001).
- [36] T. Stantcheva, V. I. Shematovich, and E. Herbst, *Astron. Astrophys.* **391**, 1069 (2002).
- [37] T. Stantcheva and E. Herbst, *Mon. Not. R. Astron. Soc.* **340**, 983 (2003).
- [38] D. T. Gillespie, *J. Chem. Phys.* **115**, 1716 (2001).
- [39] H. Salis and Y. N. Kaznessis, *J. Chem. Phys.* **123**, 214106 (2005).
- [40] Y. Cao, D. T. Gillespie, and L. R. Petzold, *J. Chem. Phys.* **124**, 044109 (2006).
- [41] A. Lipshtat and O. Biham, *Phys. Rev. Lett.* **93**, 170601 (2004).
- [42] B. Barzel, O. Biham, and R. Kupferman, *Phys. Rev. E* **76**, 026703 (2007).
- [43] B. Barzel, O. Biham, and R. Kupferman, *Multiscale Model. Simul.* **6**, 963 (2007).
- [44] A. Lipshtat and O. Biham, *Astron. Astrophys.* **400**, 585 (2003).
- [45] B. Barzel and O. Biham, *Astrophys. J.* **658**, L37 (2007).
- [46] B. Barzel and O. Biham, *J. Chem. Phys.* **127**, 144703 (2007).
- [47] C. A. Gómez-Urbe and G. C. Verghese, *J. Chem. Phys.* **126**, 024109 (2007).
- [48] E. L. Haseltine and J. B. Rawlings, *J. Chem. Phys.* **117**, 6959 (2002).
- [49] J. Puchalka and A. M. Kierzek, *Biophys. J.* **86**, 1357 (2004).
- [50] K. Vasudeva and U. S. Bhalla, *Bioinformatics* **20**, 78 (2004).
- [51] U. Kummer, B. Krajnc, J. Pahle, A. K. Green, C. J. Dixon, and M. Marhl, *Biophys. J.* **89**, 1603 (2005).
- [52] O. Biham, I. Furman, N. Katz, V. Pirronello, and G. Vidali, *Mon. Not. R. Astron. Soc.* **296**, 869 (1998).
- [53] O. Biham and A. Lipshtat, *Phys. Rev. E* **66**, 056103 (2002).
- [54] J. Krug, *Phys. Rev. E* **67**, 065102(R) (2003).
- [55] I. Lohmar and J. Krug, *Mon. Not. R. Astron. Soc.* **370**, 1025 (2006).
- [56] H. Cuppen and E. Herbst, *Astrophys. J.* **668**, 294 (2007).
- [57] D. A. Williams, T. W. Hartquist, and D. C. B. Whittell, *Mon. Not. R. Astron. Soc.* **258**, 599 (1992).